

$$\varepsilon = \frac{\ln \left( \frac{Q}{\frac{\pi}{4} \left[ W_0 + \frac{H}{H_t} (W_t - W_0) \right]^2} \right) - \ln \left( 10^{\frac{-L\gamma}{W_0 + \frac{H}{H_t} (W_t - W_0)}} \left( \frac{4(\rho_p - \rho)^2 g^2}{225 \rho \mu} \right)^{\frac{1}{3}} (L\gamma) \right)}{4.4 \left[ \frac{\rho (L\gamma)^2}{\mu} \left( \frac{4(\rho_p - \rho)^2 g^2}{225 \rho \mu} \right)^{\frac{1}{3}} \right]^{-0.1}} \quad (32)$$

After using equation (32) to eliminate  $\varepsilon$ , only the variable  $G$  remains to be eliminated from equation (22). This variable gives the reaction rate, expressed as the layer thickness precipitated onto a particle surface per unit time. Shiau and Liu (1998) expressed the reaction rate in this form, first recognizing that the molar rate of consumption of struvite (moles struvite per volume of solution per time) times the density of struvite gives the volume of struvite precipitated per time per volume of liquid. Then, dividing this struvite volume precipitation rate by the surface area available for precipitation in that same volume of liquid yields the reaction rate in the desired form. In the present case, Equation (10), rather than the more generic rate equation used by Shiau and Liu (1998), gives the molar rate of consumption per time ( $dx/dt$ ), therefore:

$$\frac{\text{vol. struvite}}{(\text{time})(\text{vol. solution})} = \frac{mk'(P - P_e)}{3x^2 - 2([M]_0 + [A]_0 + [P]_0)x + ([M]_0[A]_0 + [A]_0[P]_0 + [P]_0[M]_0)} \rho_p \quad (33)$$

The volume of bed particles available per volume of solution is equal to  $\varepsilon/(1-\varepsilon)$ , and multiplying this by the surface-to-volume ratio of the bed particles ( $\alpha L^3/\beta^2$ , or  $\alpha L/\beta$ ), gives the surface area available for precipitation per volume of solution. As in the Shiau and Liu (1998) method, this product is then divided into the right side of equation (33) to yield an expression for  $G$ :

$$G = \frac{mk'(P - P_e)}{3x^2 - 2([M]_0 + [A]_0 + [P]_0)x + ([M]_0[A]_0 + [A]_0[P]_0 + [P]_0[M]_0)} \frac{\rho_p}{\left( \frac{1-\varepsilon}{\varepsilon} \right) \left( \frac{\beta}{\alpha L} \right)} \quad (34)$$

Equation (34) contains  $x$  in the denominator, and writing out  $P$  as in equation (4) introduces  $x$  into the numerator as well, while this variable does not occur in the Shiao and Liu (1998) method. However, in dilute solutions, the molarity of struvite is approximately equal to 7.331 times the weight fraction of struvite (because each mole is 1/7.331 of a kilogram), and therefore the variable  $x$  can be equated to  $7.331(C-C_0)$ . Substituting this expression in the present case thus removes  $x$ , yielding:

$$G = \frac{mk' \{ ([M]_0 - 7.331[C - C_0])([A]_0 - 7.331[C - C_0])([P]_0 - 7.331[C - C_0]) - P_e \} \rho_p \left( \frac{\varepsilon}{1 - \varepsilon} \right) \left( \frac{\alpha L}{\beta} \right)}{3(7.331[C - C_0])^2 - 2([M]_0 + [A]_0 + [P]_0)(7.331[C - C_0]) + ([M]_0[A]_0 + [A]_0[P]_0 + [P]_0[M]_0)} \quad (35)$$

We now have our desired mathematical relation for  $(dC/dH)$ , as all variables in equation (22) other than  $C$ ,  $L$ , and  $H$  have now themselves been expressed in terms only of constants and  $C$ ,  $L$ , and  $H$ .

The relation is expressed by equation (22), where  $A$ ,  $\varepsilon$ , and  $G$  are given by equations (23), (32), and (35), respectively.

The second material balance equates the time rate of mass increase of growing particles within a horizontal slice of the crystallizer to the time rate of mass increase in particles as calculated by subtracting the particle mass entering the slice from that exiting the slice:

$$\rho_{p^*} N \alpha (L^3_H - L^3_{H+\Delta H}) = \frac{(1 - \varepsilon) \left[ \frac{1}{3} \pi \Delta H (r_H^2 + r_H r_{H+\Delta H} + r_{H+\Delta H}^2) \right]}{(\alpha L^3)} \beta L^2 G \rho_{p^*} \quad (36)$$

The right side of the equation represents the time rate of mass increase of particles within the slice, the same expression used for that quantity in equation (20). The left side represents the particle mass rate difference between exiting and entering particles, and can be broken into three factors:

$\alpha(L^3_H - L^3_{H+\Delta H})$ , the volume difference per particle between the particles exiting the slice at the bottom and those entering at the top;

$N$  , the number of particles entering and exiting the slice (same as seeding rate); and

$\rho_{p^*}$  , the mass of Mg, ammonium, and phosphate ions per volume of solid struvite.

Now, rearranging equation (36):

$$\frac{(L^3_H - L^3_{H+\Delta H})}{\Delta H} = \frac{(1-\varepsilon) \left[ \frac{1}{3} \pi (r_H^2 + r_H r_{H+\Delta H} + r_{H+\Delta H}^2) \beta G \right]}{N \alpha^2 L} \quad (37)$$

Taking the limit as  $\Delta H$  approaches zero, and substituting  $A$  as in equation (22):

$$\frac{dL^3}{dH} = \frac{(1-\varepsilon) [A \beta G]}{N \alpha^2 L} \quad (38)$$

Now,  $L^3$  is a function of  $L$ , and therefore from the chain rule for differentiation we know that:

$$\frac{dL^3}{dH} = 3L^2 \frac{dL}{dH} \quad (39)$$

Substituting equation (36) into (35) and rearranging results in:

$$\frac{dL}{dH} = \frac{(1-\varepsilon) [A \beta G]}{3N \alpha^2 L^3} \quad (40)$$

The only variables in equation (40) other than  $C$ ,  $L$ , and  $H$  are  $\varepsilon$ ,  $A$ , and  $G$ . However, the latter three can be expressed by equations (32), (23), and (35), respectively. Therefore, we now have a relation for  $(dL/dH)$  in terms only of constants and of  $C$ ,  $L$ , and  $H$ . This relation and the relation derived above for  $(dC/dH)$ , which together constitute the PLCB model, are summarized in Appendix A.

As can be seen in Figure 11, in this model the concentration profile drops continuously from the point of entry of the liquid to the top of the reaction zone. The conditions for this profile were the same set as that described for the profiles of the MLMB and PLMB models, except that the bed characteristics are predicted by the model in this case rather than treated as input, and the seed size, seeding rate, and struvite product size are used as input.

To produce the profile, the initial conditions, that is, the values for  $C$  and  $L$  at the bottom of the reaction zone ( $H = 0$ ) are used in the two differential equations defining the model. The value for  $C$  at the bottom corresponds with the raw liquid composition, and the value for  $L$  is the radius of the product struvite. The two equations yield the slopes of  $C$  and  $L$  with respect to  $H$ . The slopes are applied to a small increment (0.05 cm) of  $H$  to calculate  $C$  and  $L$  at a height of 0.05 cm. The equations are used to calculate the slopes again, and the process is repeated until the height at which  $L$  has dropped to the diameter of the seeds. The bed top occurs at this height, and the process is terminated. The values for  $C$ , which are expressed in kg struvite per kg water, are converted to ppm phosphorus by multiplying by one million and by the ratio of the atomic weight of phosphorus to the molecular weight of struvite.

Because the bed particle diameter increases toward the bottom of the zone in this model, and because surface area available for reaction per mass of bed decreases as particle diameter increases, the point of sharpest decrease in concentration does not occur immediately after the point of entry but rather is delayed in comparison with the PLMB model. Also, the PLCB model predicts a bed of varying density, which also affects the profile. For example, the predicted bed density is often lowest at the bottom of the reaction zone, resulting in further slowing of the reaction there in comparison with PLMB.

Another characteristic of the PLCB model is that, consistent with the assumption of perfect bed classification, it predicts smallest particle size, and hence greatest surface area available for reaction, in the upper portion of the reaction zone. Because the upper portion is of greater diameter, the upward velocity is slower there, and hence the liquid spends a greater portion of its time in an area rich in surface area. The result is that concentration drops more rapidly there in comparison with the other two models.

## Comparison of the Models

Figure 11 illustrates how dissolved OP is predicted by the three models to drop with respect to height for the same reactor under the same conditions. The conditions were chosen to illustrate differences among the models, especially ultimate reduction achieved. It should be noted that if a faster rate constant were assumed, or conditions were chosen to allow greater residence time and/or greater surface area due to a finer or more massive bed, all three models would yield a closer approach to equilibrium. In the extreme, all three models predict OP removal nearly to equilibrium, though the shape of the approach remains different.

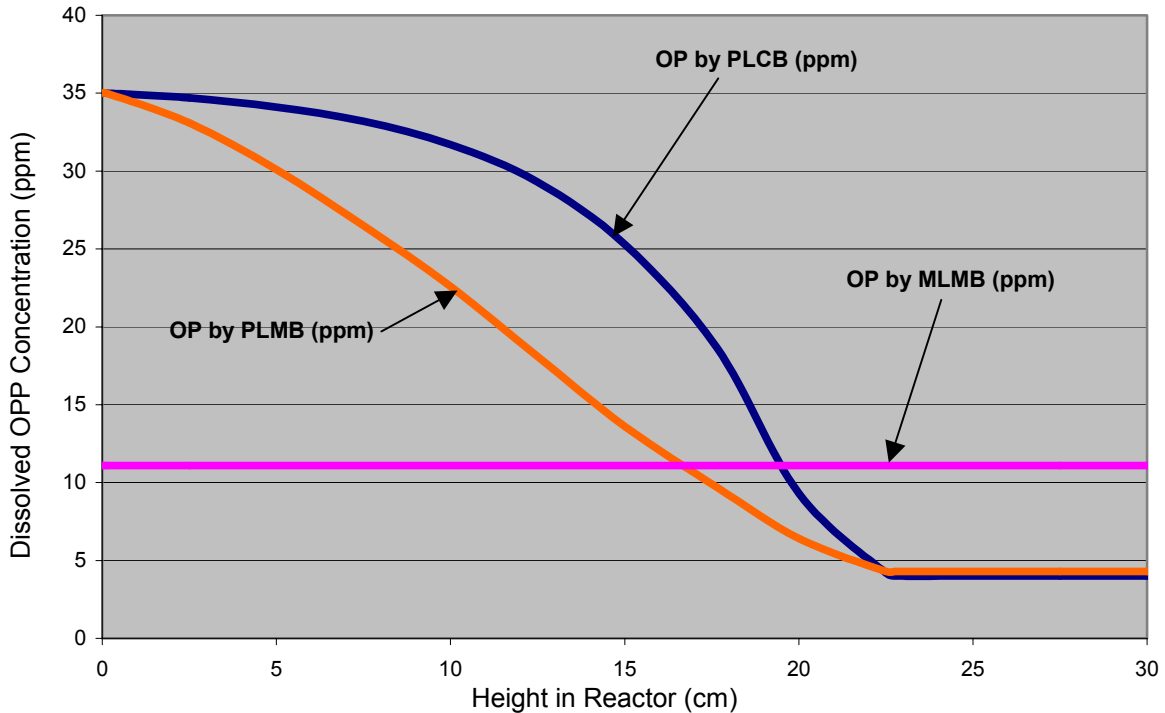


**Figure 11: Dissolved OP Concentration (ppm) versus Height (cm) in Reactor, Predicted by Three Models**

For Figure 11, the reactor is a cone of 2.54 cm (1 in.) diameter at the bottom, expanding to 17.8 cm (7 in) at a height of 61 cm (two feet). The liquid flow rate is 21.5 L/h, and dissolved in the liquid after Mg and pH augmentation are 35 ppm OP, 60 ppm Mg, and 600 ppm TAN at a pH of 8.4. The reaction constant is assumed to be 0.25 dm/h.

For the PLCB model, seeds 0.3 mm in diameter are added to the top of the bed at a rate of 15/s, and product particle size is 0.8 mm diameter. All particles are assumed to be spherical. At these conditions, the PLCB model predicts a bed ranging in density from only 46% occupied by bed particles at the bottom (void space of 54%), rising to 64% at 13 cm height, then falling to 59% at the bed top. The bed top is predicted at 22.8 cm, and total bed surface area and volume are predicted to be 303 square dm and 0.4 L, respectively.

Note that the MLMB and PLCB models do not predict the particle size distribution, height, or mass of the bed. Rather, the characteristics of the bed are considered input data for these models. Unlike the PLCB model, the final result (OP reduction achieved) in the MLMB and PLMB models depends solely on the total surface area of the bed, regardless of the bed mass, height, or particle size distribution. In practice, the total surface area and to some extent the particle size distribution and height can be controlled toward desired values by manipulating the seeding rate and product removal timing and technique. In the present comparative analysis, the same mass, height, and particle size distribution as that predicted by PLCB was taken as input for the other two models, with the distribution homogeneous with respect to height due to the assumption of perfect bed-mixing in those two models.

In Figure 11, the PLCB profile drops very slowly at first, as the liquid moves through the bottom zone where surface area is sparse due to large particle size and low bed density. The reaction then speeds up, due to smaller particle size, greater density, and slower upward velocity allowing greater time in contact with high surface area. The result is OP removal of 91%.

The PLMB profile begins dropping more rapidly at first than the PLCB because its bed is finer and denser at the bottom than that of the latter. However, by the mid-level, the trend reverses itself because the PLMB bed is coarser at the top than the PLCB bed. The net result is that OP reaches the same value as that achieved by PLCB.

The MLMB profile is flat at the final value due to the assumption that both bed and liquid are perfectly mixed. In this scenario, the ultimate removal is limited by the fact that entering, high-OP liquid is mixed into the liquid exiting the reaction zone. The result is OP removal of only 68%.